THE ASTROPHYSICAL JOURNAL, 185:577–596, 1973 October 15

ULTRAVIOLET PHOTOMETRY FROM THE ORBITING ASTRONOMICAL OBSERVATORY. VIII. THE BLUE Ap STARS

DAVID S. LECKRONE
National Aeronautics and Space Administration, Goddard Space Flight Center, Greenbelt, Maryland
Received 1973 January 15; revised 1973 April 30

ABSTRACT

The Wisconsin Experiment Package filter photometers on OAO-2 were used to obtain data for a carefully selected set of 24 blue ($B - V < 0.00$) Ap stars and 31 comparison standard B and A dwarfs and giants for a program of relative photometry over the effective wavelength range 1430–4250 Å. The Ap stars observed include members of the Si, Hg-Mn, and Sr-Cr-Eu peculiarity classes, and most of them are too blue in $B - V$ for their published MK spectral classes. The close similarity, deduced from ground-based observations, between the blue Ap stars and normal B stars of similar *UBV* colors is not maintained in the ultraviolet. The blue Ap stars emit less ultraviolet flux than normal stars of like *UBV* colors. They are underluminous and cool in effective temperature for their colors. The Hg-Mn stars are less flux-deficient in the ultraviolet, for their *UBV* colors, than are Si and Sr-Cr-Eu stars. In most cases the ultraviolet flux distribution of a blue Ap star closely resembles that of a normal star of similar MK spectral class. These results are confirmed by ultraviolet spectrophotometry at 10 and 20 Å resolution of the Si star θ Aur, data also obtained with OAO-2. Interesting differences in detail between θ Aur and normal stars are evident in the latter data. The possible role of enhanced ultraviolet opacities in modifying the shape of the emergent flux envelope of an Ap star and in modifying its atmospheric structure, relative to normal B stars, is discussed.

Subject headings: peculiar A stars — spectrophotometry — ultraviolet

I. INTRODUCTION

It has long been known that many of the peculiar A and B stars (hereinafter designated Ap stars) are too blue for their spectral types (Deutsch 1947). This is particularly true for the silicon stars, some of which are as blue as $(B - V) = -0.19$, while being classified as late as B9 or A0 on the MK system. Deutsch (1947) suggested that such stars possess the gross characteristics of normal main-sequence B stars of similar color and that their spectral types of late B to early A result from the suppression of the He I lines, which serve as B-type spectral class indicators, by some unknown mechanism. This inference has received extensive support over the past decade. For example, studies by Searle and Sargent (1964), Mihalas and Henshaw (1966), and Jugaku and Sargent (1968) indicate that the blue ($B - V < 0.00$) Ap stars possess Balmer line strengths, Balmer discontinuities, and Si III/Si II line-strength ratios which are consistent with their *UBV* colors. In addition, blue Ap stars belonging to open clusters occupy positions normal for their *UBV* colors in the cluster color-magnitude diagrams (Hyland 1967). Evidence of this sort has led to almost universal acceptance of the viewpoint that a blue Ap star possesses the mass, luminosity, and atmospheric structure at depth of a normal main-sequence B star with the same *UBV* colors and that any discordance between its colors and its MK spectral type is the accidental result of an atmospheric deficiency of helium (Sargent and Searle 1967). Important corollaries to this conclusion are that the strong Ap star magnetic fields do not affect in any observable way the structure of their deeper atmospheric layers and that abnormal elemental abundances derived from weak spectral lines, observed at visible wavelengths, reflect

real photospheric abundance anomalies rather than a peculiar temperature-pressure distribution.

The B stars emit a substantial fraction of their flux at wavelengths shorter than 3000 Å. The general view of the blue Ap stars outlined above must therefore be regarded as incomplete until their ultraviolet flux distributions have been taken into account. That Ap star phenomena observed in the visible may be fundamentally related to phenomena observable in the ultraviolet has been amply demonstrated in several recent studies. Peterson (1970) and Wolff and Wolff (1971) suggest that variable continuous or line opacity sources at ultraviolet wavelengths may drive the photometric variability observed in the visible. The pioneering study of α^2 CVn from OAO-2 by Molnar (1973) strongly supports this idea. Strom and Strom (1969) have emphasized that a star of high silicon abundance may imitate in its *UBV* colors and Balmer discontinuity a normal star of hotter effective temperature, due to enhanced ultraviolet Si I continuous absorption. Although they undoubtedly overestimated the relative importance of Si I by ignoring other potentially important opacity sources (Peterson 1970), including the wing of the H I Lα line (Klinglesmith 1972), the central idea developed by Strom and Strom merits further investigation. Using OAO-2 data, Code (1969) noted that the Si star θ Aur is flux deficient at 1700 Å for its $B - V$ color, as compared with normal stars. Similarly in their study of "helium-weak" stars Bernacca and Molnar (1972) found three probable Ap stars which appear flux deficient at 1910 and 2460 Å.

The present study represents the first comprehensive ultraviolet photometric survey of the blue Ap stars. Its principal aim is to determine whether the close similarity discussed above between the blue Ap stars and normal B stars with similar *UBV* colors is maintained at wavelengths shortward of 3000 Å. Data are presented for 24 Ap stars and 31 normal comparison standard dwarfs and giants, observed with the Wisconsin Experiment Package (WEP) on OAO-2 (Code *et al.* 1970). Both normal and peculiar stars were chosen, with a few exceptions, for their minimal interstellar reddening and for the absence of known bright companions. Emphasis has been placed on the reduction of all the data to a self-consistent photometric system.

II. THE STARS OBSERVED

Table 1 summarizes pertinent data for the Ap stars observed, while data for the normal comparison standards are given in table 2. In most cases spectral peculiarities adopted in table 1 represent a consolidation of peculiarity classes assigned by Osawa (1965) and by Cowley *et al.* (1969). Differences between these two sources are typically minor. Most of the Ap stars and most of the normal late B and early A stars considered here have been classified in a consistent way on the MK system by Cowley *et al.* (1969). The *UBV* colors of Johnson *et al.* (1966) were adopted wherever possible. Unfortunately, the latter source provides colors for only one third of the Ap stars of interest and had to be supplemented by data from Stępień (1968*b*) and from Eggen (1967).

Except for HD 184905, all of the stars observed possess color excesses $E(B - V) \leq 0.03$ relative to the Johnson (1963) standard main sequence. A large majority of them have $E(B - V) \leq 0.02$. In dealing with color excesses this small, it is difficult to separate the effects of genuine interstellar reddening from the uncertainties in the *UBV* data or from possible small intrinsic differences between the $(U - B)$ versus $(B - V)$ relations for normal and Ap stars. In the present study, stars with $E(B - V) \leq 0.02$, including all the Ap stars except HD 184905, were assumed to be totally unreddened. Data for normal stars with $E(B - V) = 0.03$ were corrected for reddening, by use of the "average" extinction curve of Bless and Savage (1972), only if that correction brought their ultraviolet flux distributions into closer agreement with those of other stars of the same spectral type, possessing smaller color excesses. This rather arbitrary procedure resulted in small reddening corrections being adopted for HR 2154 and

TABLE 1

PECULIAR STARS OBSERVED

HD	Name or HR	Spectral Peculiarity	Pec. Source*	V	$B-V$	$U-B$	UBV Source*	Remarks†
358...	α And	Hg, Mn	*a, b*	2.06	−0.11	−0.47	*e*	SB1, VB(9.2)
10783...	...	Cr, Sr	*a*	6.56	−0.06	−0.16	*g*	
25267...	τ^9 Eri	Si 3955	*a*	4.66	−0.14	−0.41	*e*	SB1
32650...	1643	Si 3955, Eu	*a, b*	5.44	−0.12	−0.36	*f*	
33904...	μ Lep	Hg, Mn	*a, b*	3.29	−0.11	−0.39	*e*	
34452...	1732	Si 4200	*a, b*	5.35	−0.19	−0.62	*f*	
39317...	137 Tau	Si, Cr	*a, b*	5.55	−0.06	−0.07	*f*	
40312...	θ Aur	Si 3955	*a, b*	2.62	−0.08	−0.18	*e*	VB(4.5)
68351...	15 Cnc	Si 3955, Cr	*a, b*	5.63	−0.08	−0.12	*g*	SB1
74521...	49 Cnc	Si 3955, Cr, Eu‡	*a, b*	5.65	−0.10	−0.24	*g*	
78316...	κ Cnc	Hg	*a*	5.23	−0.11	−0.44	*g*	SB1
89822...	4072	Hg, Mn§	*a, c, d*	4.99	−0.07	−0.15	*e*	SB2
112413...	α^2 CVn	Si, Hg, Eu, Cr	*a, b*	2.89	−0.12	−0.32	*e*	VB(2.7)
120198...	84 UMa	Eu, Cr	*a, b*	5.66	−0.05	−0.15	*f*	
133029...	5597	Si 3955, Sr, Cr	*a, b*	6.37	−0.10	−0.26	*f*	VB(3.2)
143807...	ι CrB	Hg	*a, b*	4.98	−0.07	−0.20	*e*	
144206...	υ Her	Hg, Mn	*a, b*	4.76	−0.11	−0.32	*e*	
149822...	6176	Si, Cr, Sr	*a, b*	6.38	−0.08	−0.19	*f*	
173524...	46 Dra	Hg, Mn	*a, b, c*	5.05	−0.12	−0.30	*f*	SB2
183056...	4 Cyg	Si	*a, b*	5.16	−0.12	−0.41	*f*	SB1
184905...	...	Si, Cr, Sr	*a*	6.43	−0.09	−0.27	*f*‖	
196178...	7870	Si 4200	*a, b*	5.77	−0.15	−0.54	*f*	
199728...	20 Cap	Si 4200	*b*	6.23	...	...	#	
223640...	108 Aqr	Si 4200, Sr, Cr	*a, b*	5.17	−0.16	−0.45	*f*	

* SOURCE.—*a*, Osawa 1965; *b*, Cowley *et al.* 1969; *c*, Conti 1970; *d*, Dworetsky 1972; *e*, Johnson *et al.* 1966; *f*, Eggen 1967; *g*, Stępień 1968*b*.

† SB1, SB2 denote single- or double-lined spectroscopic binaries (Abt and Snowden 1973). VB(Δm) denotes visual binaries with magnitude differences taken from Blanco *et al.* 1968 or Hoffleit 1964.

‡ Classified as Eu, Cr by Cowley *et al.* 1969.

§ Classified as Si (Sr, Hg) by Cowley *et al.* 1969.

‖ Corrected for interstellar extinction, $E(B-V) = 0.06$.

V from Hoffleit 1964. $U-V \approx -0.53$ estimated from $-2.5 \log F(4250\ \text{Å})$ vs. $U-V$ relation for unreddened Si stars.

δ Per. If any of the stars assumed to be unreddened here were in fact reddened by $E(B-V) = 0.02$, its *normalized* flux distribution, derived as discussed in § III, would be in error by about 0.07 mag, near 1900 Å. It must be emphasized that such uncertainties are small compared with the intrinsic differences among stars discussed in subsequent sections.

Nearly half of the stars listed in tables 1 and 2 are binaries. However, visual binaries with magnitude differences $\Delta V < 2.5$ and double-lined spectroscopic binaries, with two exceptions, have been excluded. No attempt has been made to correct either *UBV* colors or ultraviolet apparent magnitudes of a given star for the possible presence of faint companions, such procedures being strongly subject to error. The normalized absolute flux scale discussed in § III is defined relative to unity flux at 3320 Å. A faint companion which contributes a few hundredths of a magnitude to the apparent brightness at 3320 Å and which makes no measurable contribution below 2000 Å will cause measured brightnesses below 2000 Å to appear relatively *too faint* by a few hundredths of a magnitude. Because stars with known bright companions have been avoided, such distortions of the normalized flux distributions hopefully have been minimized.

TABLE 2

NORMAL STARS OBSERVED

HD	Name or HR	MK Spectral Class	MK Class Source*	V	$B-V$	$U-B$	*UBV* Source*	Remarks†
14055.....	γ Tri	A1 V	*b*	4.01	+0.02	+0.02	*d*	
15008.....	δ Hyi	A2 V	*a*	4.09	+0.03	+0.05	*d*	
16978.....	ϵ Hyi	B9 III–V	*a*	4.11	−0.06	−0.14	*d*	
17081.....	π Cet	B7 V	*a*	4.25	−0.14	−0.45	*d*	
22928.....	δ Per	B5 III	*a*	2.92	−0.15	−0.53	*d*‡	SB1
23227.....	δ For	B5 IV	*c*	5.00	−0.16	−0.60	*d*	
24626.....	1214	B6 V	*c*	5.11	−0.13	(−0.52)	*d*§	
32630.....	η Aur	B3 V	*a*	3.18	−0.18	−0.67	*d*	
33802.....	ι Lep	B8 V	*a*	4.44	−0.09	−0.40	*d*	VB(6.3)
33949.....	κ Lep	B8 III–V	*a*	4.36	−0.10	−0.34	*d*	VB(2.9)
34759.....	ρ Aur	B5 V	*a*	5.22	−0.15	−0.58	*e*	SB1
37795.....	α Col	B8 Ve	*a*	2.64	−0.12	−0.46	*d*	VB(8.7)
38899.....	134 Tau	B9.5 V	*b*	4.91	−0.07	−0.16	*d*	
39844.....	ϵ Dor	B6 V	*c*	5.11	−0.14	−0.49	*d*	
41692.....	2154	B5 IV	*a*	5.29	−0.16	−0.56	*d*‡	VB(6.2)
45796.....	2360	B6 V	*c*	6.26	−0.13	(−0.48)	*d*§	
47105.....	γ Gem	A1 IV	*b*	1.92	0.00	+0.05	*d*	SB1
58715.....	β CMi	B8 V	*a*	2.89	−0.09	−0.27	*d*	
70011.....	λ Cnc	B9.5 V	*b*	5.91	−0.03	−0.12	*e*	
74198.....	γ Cnc	A1 IV	*b*	4.66	+0.02	+0.01	*d*	SB1
74280.....	η Hya	B3 V	*a*	4.30	−0.20	−0.74	*d*	SB1
82621.....	26 UMa	A2 V	*b*	4.51	0.00	+0.04	*d*	
95418.....	β UMa	A1 V	*b*	2.37	−0.02	0.00	*d*	
103287.....	γ UMa	A0 V	*b*	2.44	0.00	+0.03	*d*	SB1
106591.....	δ UMa	A3 V	*b*	3.31	+0.08	+0.07	*d*	
123299.....	α Dra	A0 III	*b*	3.65	−0.05	−0.08	*d*	SB1
147394.....	τ Her	B5 IV	*a*	3.90	−0.15	−0.56	*d*	VB(10.7)
160762.....	ι Her	B3 V	*a*	3.80	−0.18	−0.69	*d*	SB1
161868.....	γ Oph	A0 V	*b*	3.75	+0.04	+0.04	*d*	
186882.....	δ Cyg	B9.5 III	*b*	2.87	−0.02	−0.10	*d*	VB(4.9) SB1
193432.....	ν Cap	B9.5 V	*b*	4.76	−0.04	−0.11	*d*	VB(7.0)
201908.....	77 Dra	B8 V	*b*	5.92	−0.08	−0.24	*f*	
222173.....	ι And	B8 V	*a*	4.29	−0.11	−0.29	*d*	SB1

* SOURCE.—*a*, Jaschek *et al.* 1964; *b*, Cowley *et al.* 1969; *c*, Hiltner *et al.* 1969; *d*, Johnson *et al.* 1966; *e*, Blanco *et al.* 1968; *f*, Stępień 1968*a*.

† Notation and visual binary data sources same as for table 1. Spectroscopic binary data from Hoffleit 1964, Jaschek *et al.* 1964, or Batten 1967.

‡ Corrected for interstellar extinction, $E(B-V) = 0.03$.

§ $U-B$ estimated from $-2.5 \log F(4250\ \text{Å})$ vs. $U-B$ relation for normal unreddened stars.

The Hg-Mn stars HR 4072 and 46 Dra are of sufficient interest to be included here even though both are double-lined spectroscopic binaries. According to Conti (1970) both components of 46 Dra are Hg or Hg-Mn stars and they are similar in mass and effective temperature. Thus, the data given below for 46 Dra represent the composite of two very similar stars and a correction of *UBV* colors or ultraviolet flux distributions is unnecessary. A $\Delta V = 1.7$ mag difference exists between the components of HR 4072, the brighter of which is also a Hg-Mn star (Conti 1970). The fainter companion may depress the apparent *normalized* flux distribution of HR 4072 by as much as 0.10–0.15 mag in the far ultraviolet, while causing the composite $U-V$ color to be about 0.07 mag larger than that of the bright component alone. The simultaneous correction of the ultraviolet data and the *UBV* colors of HR 4072 produces no qualitative change in the results for Hg-Mn stars reported below.

III. THE PHOTOMETRY

The OAO-2 spacecraft and the Wisconsin Experiment Package functioned about four times longer than originally expected. Most of the observations reported here were carried out well after the nominal experiment lifetime had been exceeded. Fortunately, the long-term variations in photometer response were relatively smooth and well defined.

The present observations were obtained with the seven broad-band filters listed in table 3, the most reliable WEP filters. An apparent stellar magnitude at effective wavelength λ and at a given epoch of observation is defined by

$$m(\lambda) = -2.5 \log \left(\frac{s + \delta s - d}{c - d} - \frac{b - d}{c - d} \right)_{\lambda} . \quad (1)$$

Here s, b, c, and d are digital counts in a given exposure time obtained for the star, the sky background, the on-board calibration source, and the photometer dark current, respectively. The correction for pulse counter nonlinearity, δs, has been derived from plots of digital counts versus analog voltage and has proven to be independent of the epoch of observation. This nonlinearity correction is important for stars brighter than $B \approx 4.5$, but then typically only for the 4250 Å bandpass. Only for the very brightest stars observed does it become significant at other wavelengths. Nonlinearity corrections are uncertain by about ± 0.03 mag.

To account for variations in $m(\lambda)$ with time, due primarily to filter degradation and to the radioactive decay of the calibration source, one determines a correction term $\delta m(\lambda)$ which reduces $m(\lambda)$ to the system defined by the sensitivity of the photometers at orbit 8000. Hereinafter the discussion will deal with apparent magnitudes reduced to orbit 8000, given by

$$m'(\lambda) = m(\lambda) - \delta m(\lambda) . \quad (2)$$

The $\delta m(\lambda)$ corrections have been determined for each filter as a function of time and stellar spectral class by following variations in the data for 32 B3 to A3 dwarfs and giants, each of which was observed at least twice during the life of the spacecraft. Many of the normal stars listed in table 2 are included in this group. The $\delta m(\lambda)$ corrections for filters at 4250, 3320, 2980, and 2460 Å are typically less than 0.1 mag, with an uncertainty of ± 0.01 mag, and are independent of spectral class over the range B3–A3. The 1910 Å filter degraded by nearly 0.5 mag after orbit 10,000, but its degradation is smooth and well defined to within ± 0.01 mag and is independent of spectral class over the interval B3–A3. The bandpasses at 1550 and 1430 Å diminished

TABLE 3

WEP FILTER CHARACTERISTICS

Photometer (S) Filter (F)	λ (Å)*	$\delta\lambda$ (Å)†	$-2.5 \log \Delta$‡
S1 F3	4250	860	+1.705
S1 F1	3320	520	0.000
S1 F4	2980	410	−0.310
S3 F2	2460	360	−2.039
S3 F1	1910	260	−4.101
S4 F1	1550	270	−5.285
S4 F3	1430	240	−5.540

* Effective wavelength for constant energy source.

† Bandwidth at 0.5 maximum sensitivity.

‡ Preliminary relative absolute calibration factors (Code 1971).

in sensitivity by as much as 2 mag after orbit 9000. The $\delta m(\lambda)$ corrections for the 1550 Å filter are a weak function of spectral class, while those at 1430 Å depend strongly on spectral class. In the reduction of 1550 and 1430 Å data for a blue Ap star, $\delta m(\lambda)$ corrections appropriate to the stars' *UBV* colors were first applied. The star was then reclassified on the basis of its overall ultraviolet flux distribution, as discussed in § IV, and where necessary new $\delta m(\lambda)$ corrections were applied, consistent with that classification. The basic validity of this approach is an assumption of the present study. Situations where the procedure led to an ambiguous choice of $\delta m(\lambda)$ are reflected by large uncertainties in the data given in table 4 below. The uncertainties in the 1550 and 1430 Å data, though often large by ground-based standards, are small compared with the intrinsic differences among stars discussed in later sections and in no case are such uncertainties large enough to alter qualitative results obtained here. Full details about properties of the WEP photometers discussed above may be obtained directly from the author.

The scatter of individual observations about the mean $\delta m(\lambda)$ versus time relations provides a good estimate of the random errors in the data. On the average, $m'(\lambda)$ values derived for all bandpasses from 4250 to 1910 Å were repeatable to about 0.02 mag (2σ), values at 1550 Å were repeatable to about 0.03 mag, and those at 1430 Å to about 0.04 mag.

In sections that follow normal and blue Ap stars are compared on the basis of their ultraviolet normalized absolute fluxes defined by

$$-2.5 \log F(\lambda) = m'(\lambda) - m'(3320 \text{ Å}) - 2.5 \log \Delta . \quad (3)$$

Values of $-2.5 \log \Delta$, the preliminary relative absolute calibration factors derived by Code (1971), are given in table 3. Table 4 lists values of $m'(\lambda)$, the uncertainties in $m'(\lambda)$, and values of $-2.5 \log F(\lambda)$ for 55 normal and Ap stars. The uncertainties in $m'(\lambda)$ reflect random errors, as well as uncertainties in the $\delta m(\lambda)$ and δs corrections.

The effective wavelengths utilized here are valid for a constant energy source. Model atmosphere calculations by Klinglesmith (1971*a*) indicate that these effective wavelengths differ from those pertinent to early-type stars by no more than ± 50 Å over the interval 4250–1550 Å and by no more than ± 80 Å at 1430 Å. In the absence of detailed effective wavelength corrections and because of the preliminary nature of the absolute calibration, great caution should be exercised in comparing the values of $-2.5 \log F(\lambda)$ given in table 4 to model atmospheres, for example. However, the data are entirely suitable for the program of gross relative photometry discussed in the sections that follow.

IV. COMPARISON BETWEEN NORMAL AND Ap STARS

Normalized absolute fluxes in magnitude units, $-2.5 \log F(\lambda)$, at each of four effective wavelengths (2460, 1910, 1550, and 1430 Å) are plotted versus $U - V$ for normal stars and for the various classes of Ap stars in figures 1 and 2. These plots are in effect color-color diagrams. The data for normal stars define a relatively smooth and narrow band in each diagram, with a scatter that is entirely consistent with the photometric uncertainties, residual interstellar reddening, and the presence of faint companions in some cases.

Two important properties of the blue Ap stars become apparent in figures 1 and 2. First of all, the Ap stars are markedly fainter in $-2.5 \log F(\lambda)$ at each effective wavelength than normal stars of similar $U - V$ color. This result does not depend upon the choice of normalization point at 3320 Å. Normalization to $V = 0.00$ results in relative flux deficiencies for the Ap stars at least as large as those evident in figures 1 and 2. Since the Ap stars possess absolute visual magnitudes comparable to those of normal main-sequence stars of similar *UBV* colors (Eggen 1967; Hyland 1967), their

TABLE 4

APPARENT MAGNITUDES WITH THEIR UNCERTAINTIES AND NORMALIZED ABSOLUTE FLUX DISTRIBUTIONS*

Name or HD	Effective Wavelength 4250Å	3320Å	2980Å	2460Å	1910Å	1550Å	1430Å	Name or HD	Effective Wavelength 4250Å	3320Å	2980Å	2460Å	1910Å	1550Å	1430Å
α And	...	-4.80	-4.67	...	-1.71	-0.97	-0.56	34452	-3.39	-1.84	-1.74	-0.26	+1.27	+2.35	+3.00
	...	0.04	0.04	...	0.02	0.04	0.07		0.02	0.02	0.02	0.02	0.02	0.07	0.09
	...	0.00	-0.18	...	-1.01	-1.46	-1.30		+0.16	0.00	-0.21	-0.46	-0.99	-1.10	-0.70
10783	-2.03	+0.17	+0.42	+2.07	+3.67	+5.04	+5.54	ρ Aur	-3.48	-1.94	-1.94	-0.69	+0.67	+1.36	+1.62
	0.02	0.02	0.02	0.02	0.02	0.04	0.06		0.02	0.02	0.02	0.02	0.02	0.04	0.04
	-0.50	0.00	-0.06	-0.14	-0.60	-0.42	-0.17		+0.17	0.00	-0.31	-0.79	-1.49	-1.99	-1.98
δ Hyi	-4.39	-1.93	-1.66	-0.01	+1.58	+3.14	+4.15	α Col	...	-4.18	-4.12	-2.78	-1.30	-0.57	-0.29
	0.04	0.02	0.02	0.02	0.02	0.05	0.05		...	0.04	0.04	0.04	0.02	0.05	0.03
	-0.76	0.00	-0.04	-0.12	-0.59	-0.22	+0.54		-0.05‡	0.00	-0.25	-0.64	-1.22	-1.68	-1.65
ε Hyi	-4.48	-2.33	-2.20	-0.76	+0.67	+1.52	+2.05	134 Tau	-3.72	-1.55	-1.43	-0.02	+1.41	+2.26	+2.77
	0.04	0.02	0.02	0.02	0.02	0.03	0.06		0.02	0.02	0.02	0.02	0.02	0.04	0.09
	-0.45	0.00	-0.18	-0.47	-1.10	-1.44	-1.16		-0.47	0.00	-0.19	-0.51	-1.14	-1.48	-1.22
π Cet	-4.40	-2.66	-2.60	-1.25	+0.15	+0.90	+1.20	137 Tau	-3.01	-0.65	-0.37	+1.21	+2.74	+4.08	+4.63
	0.04	0.02	0.02	0.02	0.02	0.04	0.05		0.02	0.02	0.02	0.02	0.02	0.04	0.09
	-0.04	0.00	-0.25	-0.63	-1.29	-1.73	-1.68		-0.66	0.00	-0.03	-0.18	-0.71	-0.56	-0.26
δ Per†	...	-3.96	-3.90	-2.50	-1.10	-0.39	-0.21	ε Dor	-3.61	-1.90	-1.87	-0.52	+0.91	+1.69	+1.94
	...	0.04	0.04	0.04	0.02	0.04	0.05		0.02	0.02	0.02	0.02	0.02	0.04	0.05
	+0.09‡	0.00	-0.26	-0.65	-1.34	-1.79	-1.87		-0.01	0.00	-0.28	-0.66	-1.29	-1.70	-1.70
δ For	-3.73	-2.18	-2.19	-0.92	+0.49	+1.22	+1.38	θ Aur	...	-3.73	-3.50	-1.89	-0.39	+1.07	+1.76
	0.02	0.02	0.02	0.03	0.02	0.03	0.06		...	0.02	0.02	0.02	0.02	0.04	0.05
	+0.16	0.00	-0.32	-0.78	-1.43	-1.89	-1.98		...	0.00	-0.08	-0.20	-0.76	-0.49	-0.05
24626	-3.61	-1.95	-1.95	-0.64	+0.75	+1.46	+1.66	41692†	-3.34	-1.70	-1.66	-0.33	+1.11	+1.85	+2.16
	0.02	0.02	0.02	0.02	0.02	0.04	0.09		0.02	0.02	0.02	0.02	0.02	0.04	0.09
	+0.05	0.00	-0.31	-0.73	-1.40	-1.88	-1.93		+0.08	0.00	-0.29	-0.75	-1.39	-1.82	-1.77
τ^9 Eri	-4.00	-2.25	-2.07	-0.55	+0.92	+2.00	+2.60	45796	-2.46	-0.75	-0.70	+0.62	+2.06	+2.84	+3.09
	0.04	0.02	0.02	0.02	0.02	0.05	0.05		0.02	0.02	0.02	0.02	0.02	0.04	0.13
	-0.05	0.00	-0.13	-0.34	-0.93	-1.04	-0.69		-0.01	0.00	-0.26	-0.67	-1.29	-1.70	-1.70
η Aur	...	-4.10	-4.14	-2.93	-1.59	-1.01	-0.78	γ Gem	...	-4.03	-3.77	-2.06	-0.56	+0.86	+1.65
	...	0.04	0.04	0.04	0.02	0.04	0.04		...	0.04	0.04	0.02	0.02	0.03	0.04
	+0.28‡	0.00	-0.35	-0.87	-1.59	-2.20	-2.22		-0.74‡	0.00	-0.05	-0.07	-0.63	-0.40	+0.14
32650	-3.23	-1.29	-1.17	+0.25	+1.71	+2.74	+3.33	β CMi	...	-3.72	-3.63	-2.17	-0.73	+0.07	+0.34
	0.02	0.02	0.02	0.02	0.02	0.04	0.09		...	0.02	0.02	0.02	0.02	0.05	0.04
	-0.24	0.00	-0.19	-0.50	-1.10	-1.26	-0.92		-0.29‡	0.00	-0.22	-0.49	-1.11	-1.50	-1.48
ι Lep	-4.20	-2.40	-2.34	-0.98	+0.42	+1.20	+1.51	15 Cnc	-3.03	-0.71	-0.44	+1.22	+2.72	+4.29	+4.83
	0.04	0.02	0.02	0.02	0.02	0.03	0.03		0.02	0.02	0.02	0.02	0.02	0.04	0.09
	-0.10	0.00	-0.25	-0.62	-1.28	-1.69	-1.63		-0.62	0.00	-0.04	-0.11	-0.67	-0.29	0.00
μ Lep	...	-3.50	-3.37	-1.93	-0.53	+0.31	+0.78	λ Cnc	-2.66	-0.39	-0.22	+1.23	+2.74	+3.70	+4.23
	...	0.02	0.02	0.02	0.02	0.04	0.11		0.05	0.02	0.02	0.02	0.02	0.03	0.03
	...	0.00	-0.18	-0.47	-1.13	-1.48	-1.26		-0.57	0.00	-0.14	-0.42	-0.97	-1.20	-0.92
ϰ Lep	-4.27	-2.38	-2.29	-0.88	+0.55	+1.34	+1.71	γ Cnc	-3.83	-1.41	-1.15	+0.52	+2.06	+3.61	+4.33
	0.04	0.02	0.02	0.02	0.02	0.05	0.03		0.05	0.04	0.03	0.02	0.02	0.04	0.06
	-0.19	0.00	-0.22	-0.54	-1.17	-1.57	-1.45		-0.72	0.00	-0.05	-0.11	-0.63	-0.27	+0.20

TABLE 4 (continued)

Name or HD	Effective Wavelength 4250Å	3320Å	2980Å	2460Å	1910Å	1550Å	1430Å	Name or HD	Effective Wavelength 4250Å	3320Å	2980Å	2460Å	1910Å	1550Å	1430Å
η Hya	-4.43	-3.12	-3.17	-1.99	-0.66	+0.04	+0.20	τ Her	-4.81	-3.20	-3.20	-1.89	-0.54	+0.15	+0.35
	0.04	0.02	0.02	0.02	0.02	0.04	0.05		0.04	0.02	0.02	0.03	0.03	0.04	0.04
	+0.40	0.00	-0.36	-0.91	-1.64	-2.13	-2.22		+0.10	0.00	-0.31	-0.73	-1.44	-1.94	-1.99
49 Cnc	-3.01	-0.92	-0.67	+1.04	+2.59	+4.19	+4.70	149822	-2.29	-0.08	+0.29	+2.06	+3.64	+5.23	+5.81
	0.02	0.02	0.02	0.02	0.02	0.04	0.09		0.02	0.02	0.02	0.02	0.02	0.17	0.28
	-0.39	0.00	-0.06	-0.08	-0.59	-0.18	+0.08		-0.51	0.00	+0.06	+0.10	-0.38	+0.03	+0.35
κ Cnc	-3.38	-1.65	-1.52	-0.10	+1.38	+2.35	+2.76	ι Her	-4.94	-3.53	-3.57	-2.28	-0.98	-0.35	-0.20
	0.02	0.02	0.02	0.02	0.02	0.03	0.03		0.04	0.02	0.02	0.05	0.02	0.04	0.04
	-0.03	0.00	-0.18	-0.49	-1.07	-1.29	-1.13		+0.30	0.00	-0.35	-0.79	-1.55	-2.11	-2.21
26 UMa	-4.02	-1.53	-1.26	+0.41	+1.98	+3.37	+4.17	γ Oph	-4.77	-2.31	-2.10	-0.50	+1.12	+2.35	+3.10
	0.04	0.02	0.02	0.02	0.02	0.04	0.03		0.04	0.02	0.02	0.02	0.02	0.04	0.12
	-0.79	0.00	-0.04	-0.10	-0.59	-0.39	+0.16		-0.76	0.00	-0.10	-0.23	-0.67	-0.63	-0.13
89822	-3.65	-1.42	-1.22	+0.31	+1.81	+2.91	+3.42	46 Dra	-3.64	-1.57	-1.43	+0.02	+1.48	+2.50	+2.94
	0.02	0.02	0.02	0.02	0.02	0.07	0.09		0.02	0.02	0.02	0.02	0.02	0.04	0.09
	-0.53	0.00	-0.11	-0.31	-0.87	-0.96	-0.70		-0.37	0.00	-0.17	-0.45	-1.05	-1.22	-1.03
β UMa	...	-3.73	-3.50	-1.83	-0.34	+0.96	+1.75	4 Cyg	-3.52	-1.69	-1.59	-0.15	+1.32	+2.27	+2.73
	...	0.03	0.02	0.02	0.02	0.14	0.10		0.02	0.02	0.02	0.02	0.02	0.04	0.11
	-0.68‡	0.00	-0.08	-0.14	-0.71	-0.60	-0.06		-0.13	0.00	-0.21	-0.50	-1.09	-1.33	-1.12
γ UMa	...	-3.62	-3.39	-1.76	-0.25	+1.04	+1.78	184905†	-1.96	+0.16	+0.40	+2.06	+3.56	+4.75	+5.19
	...	0.02	0.03	0.02	0.02	0.03	0.06		0.02	0.02	0.02	0.02	0.02	0.04	0.07
	-0.73‡	0.00	-0.08	-0.18	-0.73	-0.63	-0.14		-0.37	0.00	-0.09	-0.28	-0.88	-0.85	-0.68
δ UMa	-5.14	-2.65	-2.34	-0.59	+1.02	+3.08	+4.22	δ Cyg	...	-3.34	-3.14	-1.57	-0.09	+0.95	+1.45
	0.04	0.02	0.02	0.02	0.02	0.03	0.03		...	0.02	0.02	0.02	0.02	0.03	0.03
	-0.79	0.00	0.00	+0.02	-0.43	+0.45	+1.33		-0.61‡	0.00	-0.11	-0.27	-0.85	-1.00	-0.75
α^2 CVn§	...	-3.81	-3.62	-1.93	-0.43	+0.77	+1.39	ν Cap	-3.82	-1.53	-1.37	+0.12	+1.60	+2.58	+3.19
	...	0.02	0.02	0.02	0.02	0.04	0.06		0.02	0.02	0.02	0.02	0.02	0.04	0.06
	...	0.00	-0.12	-0.16	-0.72	-0.71	-0.34		-0.59	0.00	-0.15	-0.39	-0.97	-1.18	-0.82
84 UMa	-2.92	-0.67	-0.33	+1.29	+2.83	+4.28	+4.97	196178	-2.97	-1.31	-1.24	+0.17	+1.65	+2.65	+3.08
	0.02	0.02	0.02	0.02	0.02	0.04	0.10		0.02	0.02	0.02	0.02	0.02	0.04	0.11
	-0.55	0.00	+0.03	-0.08	-0.60	-0.34	+0.10		+0.05	0.00	-0.24	-0.56	-1.14	-1.33	-1.15
α Dra	-4.93	-2.56	-2.38	-0.83	+0.66	+1.72	+2.25	20 Cap	-2.42	-0.59	-0.46	+1.04	+2.53	+3.73	...
	0.04	0.02	0.02	0.02	0.02	0.04	0.05		0.02	0.02	0.02	0.02	0.02	0.08	...
	-0.67	0.00	-0.13	-0.31	-0.88	-1.01	-0.73		-0.13	0.00	-0.18	-0.41	-0.98	-0.97	...
133029	-2.37	-0.29	-0.05	+1.63	+3.16	+4.58	+5.07	77 Dra	-2.72	-0.67	-0.57	+0.81	+2.26	+3.13	...
	0.02	0.02	0.02	0.02	0.02	0.04	0.05		0.03	0.02	0.02	0.02	0.02	0.04	...
	-0.38	0.00	-0.07	-0.12	-0.65	-0.42	-0.18		-0.35	0.00	-0.21	-0.56	-1.17	-1.49	...
ι CrB	-3.63	-1.46	-1.29	+0.21	+1.70	+2.73	+3.19	108 Aqr	-3.48	-1.71	-1.59	-0.10	+1.42	+2.40	+2.93
	0.02	0.02	0.02	0.02	0.02	0.07	0.06		0.02	0.02	0.02	0.02	0.02	0.04	0.09
	-0.47	0.00	-0.14	-0.37	-0.94	-1.10	-0.89		-0.07	0.00	-0.19	-0.43	-0.97	-1.18	-0.90
υ Her	-3.90	-1.95	-1.77	-0.37	+1.12	+1.99	+2.40								
	0.04	0.02	0.02	0.02	0.02	0.04	0.05								
	-0.25	0.00	-0.13	-0.46	-1.03	-1.35	-1.19								

* For each star top row of data gives m'(λ), second row gives uncertainty in m'(λ), third row gives -2.5 log F(λ).
† -2.5 log F(λ) values corrected for reddening with average extinction law of Bless and Savage (1972).
‡ Value estimated from -2.5 log F(4250Å) vs. (U-V) relation for normal, unreddened stars.
§ Data for phase 0.0 taken from Molnar (1973) and reduced to consistency with present photometric system.

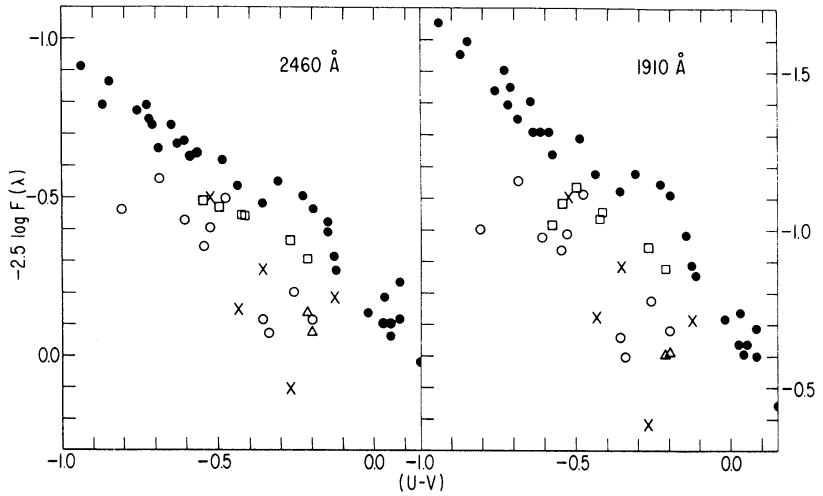

FIG. 1.—Normalized absolute fluxes in magnitude units at 2460 and 1910 Å plotted versus $U - V$ for various classes of Ap stars and for comparison standard dwarfs and giants. *Darkened circles*, normal stars. *Open circles*, Si 3955, 4200 stars. *Crosses*, other Si stars. *Open squares*, Hg-Mn stars. *Open triangles*, Sr-Cr-Eu stars. Ap stars are deficient in $-2.5 \log F(\lambda)$ compared to normal stars of similar $U - V$. Hg-Mn stars appear less flux deficient, for their $U - V$ colors, than do Si or Sr-Cr-Eu stars.

relative faintness in the ultraviolet implies that they are underluminous for their colors. Further, because the values of $-2.5 \log F(\lambda)$ are independent of the radii and distances of the stars in question, it follows from these data that $(f_\lambda/f_V)_p < (f_\lambda/f_V)_n$. Here, f_λ and f_V denote absolute fluxes emitted by unit surface area at the star, at effective wavelength $\lambda < 3320$ Å, and at the effective wavelength of the V-band, respectively. Subscripts p and n refer to a blue Ap star and a normal star, respectively, with the same intrinsic UBV colors or equivalently (Jugaku and Sargent 1968) with the same Balmer discontinuity and Paschen slope. Clearly, $(f_\lambda)_p < (f_\lambda)_n$ if $(f_V)_p \lesssim (f_V)_n$. This condition certainly holds for α^2 CVn (Molnar 1973) and for the open-cluster Si stars observed

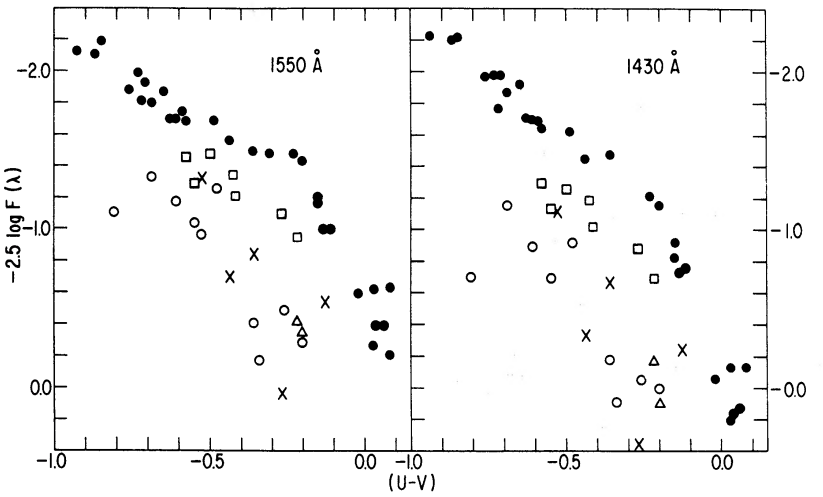

FIG. 2.—Normalized absolute fluxes in magnitude units at 1550 and 1430 Å plotted versus $U - V$ for various classes of Ap stars and for comparison standard dwarfs and giants. Symbols and description same as for fig. 1.

by Hyland (1967), contingent only on the assumption that the Ap stars possess radii not significantly smaller than normal for their *UBV* colors and absolute visual magnitudes. The latter assumption is supported by the Ap star (period, line width)-relation (Preston 1970). Moreover, ultraviolet line-blanketed and unblanketed model atmospheres which predict identical Balmer discontinuities and Paschen slopes also predict equal values of f_V to better than 1 percent, even though their ultraviolet flux distributions and effective temperatures differ significantly (e.g., Adams and Morton 1968). Thus, it appears reasonable to assume that $(f_V)_p \lesssim (f_V)_n$, and it follows that the blue Ap stars emit less ultraviolet flux and are cooler in effective temperature than normal stars with similar *UBV* colors.

Second, the Hg-Mn stars are clearly distinguishable in figures 1 and 2 from other classes of Ap stars. Compared to normal stars, the Hg-Mn stars are less flux-deficient in the ultraviolet, for their *UBV* colors, than are the Si or Sr-Cr-Eu stars. The weight of evidence from ground-based observations now supports the view that the Hg-Mn stars are innately different from other Ap stars (Preston 1971). They show no periodic variability, they have weak or nonexistent magnetic fields, they exhibit a high incidence of binary membership, and they possess smaller discrepancies between color and spectral class than do other blue Ap stars. To this accumulated evidence may now be added the fact that they are systematically brighter in the ultraviolet than other Ap stars with similar *UBV* colors.

Results of particular interest are obtained when one compares the gross ultraviolet flux distribution of an individual Ap star, defined by its $-2.5 \log F(\lambda)$ values at wavelengths ≤ 3320 Å, with comparable flux distributions of normal dwarfs and giants. The ultraviolet flux distributions of normal stars, or their ultraviolet color temperatures, vary as a relatively smooth and continuous function of MK spectral class, as may readily be confirmed by use of the data of table 4. One can estimate the MK spectral class of a normal dwarf or giant from its ultraviolet flux distribution about as well as he can on the basis of its *UBV* colors. Ambiguities of plus or minus one subclass (B9.5 being treated as a subclass equal in weight to B9 or A0) exist over the interval B5–A2. Figures 3, 4, 5, and 6 illustrate the detailed comparison of ultraviolet flux distributions of eight blue Ap stars to those of normal stars. The results of similar analyses of all 24 Ap stars treated here are summarized in table 5. Two types of normal comparison stars are shown for each Ap star—normal stars possessing *UBV* colors similar to those of the Ap star, and normal stars whose ultraviolet flux distributions *most closely match* that of the Ap star. For the sake of clarity, only a few comparison stars are illustrated in each case. The substitution of data for other normal stars listed in table 4 does not alter the results obtained.

An "ultraviolet class," defined as the MK class of the comparison stars whose ultraviolet flux distributions most closely match that of the Ap star in question, has been assigned to each Ap star in table 5. It is important to note that these ultraviolet classes are unique. A blue Ap star which, in its $-2.5 \log F(\lambda)$ values, resembles a normal early A-type star at 2460 Å, also resembles a normal early A-type star at 1910, 1550, and 1430 Å. Minor distortions of the Ap star ultraviolet flux distributions with respect to the normal stars to which they have been matched are usually of the same order as differences found among normal stars of the same MK class. In no case are such distortions large enough to render the assigned ultraviolet class ambiguous by more than one subclass.

One of the Ap stars listed in table 5, HD 149822, is clearly anomalous in its ultraviolet flux distribution as compared to other Ap stars of similar *UBV* colors and peculiarity class. It is possible, for example, that the data for this star are contaminated by a heretofore undetected bright companion. In view of this and because its 1550 Å and 1430 Å data could be reduced only in an approximate way, HD 149822 is excluded from further consideration here.

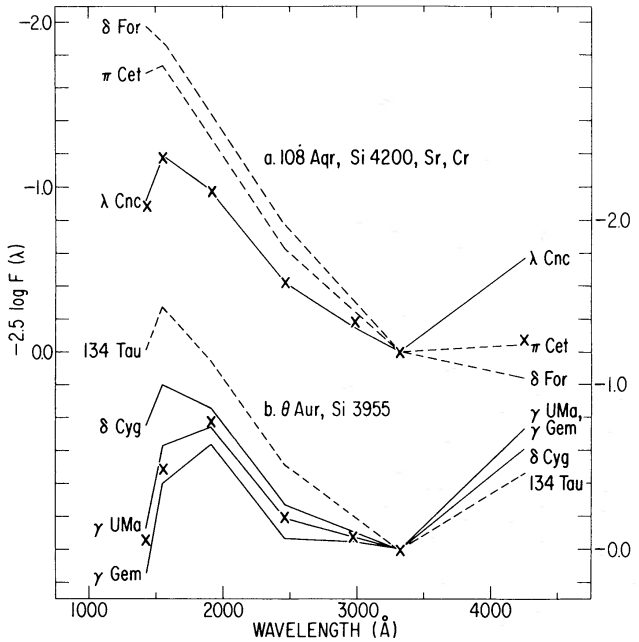

FIG. 3.—Normalized absolute flux distributions of individual Ap stars compared to those of selected normal stars. Individual data points for Ap stars are denoted by crosses. Data points for normal stars are connected by lines. Dashed lines represent normal stars with *UBV* colors similar to those of Ap star. Solid lines represent normal stars whose flux distributions at $\lambda \leq 3320$ Å most closely resemble that of Ap star. (*a*) 108 Aqr, ordinate axis labeled at left. The ultraviolet flux distribution of 108 Aqr (B9p) closely resembles that of λ Cnc (B9.5), although 108 Aqr has *UBV* colors like those of π Cet (B7) and δ For (B5). (*b*) θ Aur, ordinate axis labeled at right. θ Aur (A0p) resembles 134 Tau (B9) in its *UBV* colors but has an ultraviolet flux distribution similar to early A stars like γ UMa (A0).

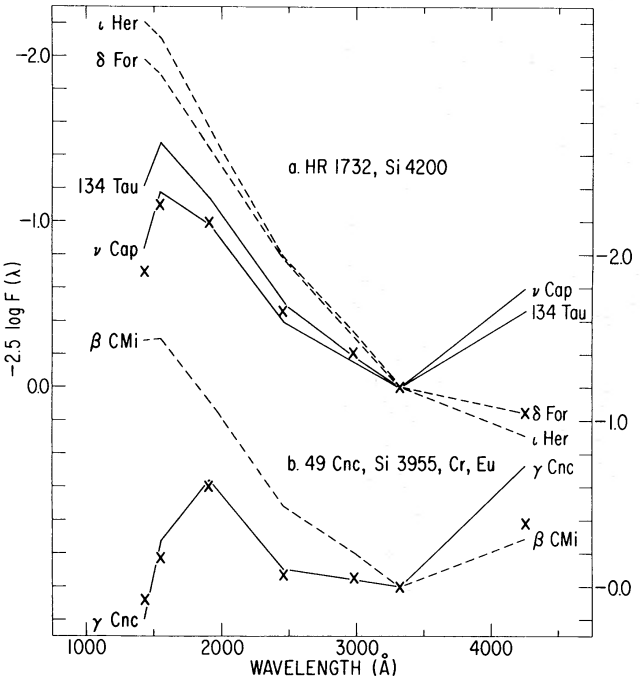

FIG. 4.—Format and symbols same as in fig. 3. (*a*) HR 1732, ordinate axis labeled at left. HR 1732 (A0p) has an ultraviolet flux distribution similar to that of ν Cap (B9.5), although its *UBV* colors resemble those of ι Her (B3) and δ For (B5). (*b*) 49 Cnc, ordinate axis labeled at right. The ultraviolet flux distribution of 49 Cnc (A1p) is nearly identical to that of γ Cnc (A1), although 49 Cnc has *UBV* colors similar to those of β CMi (B8).

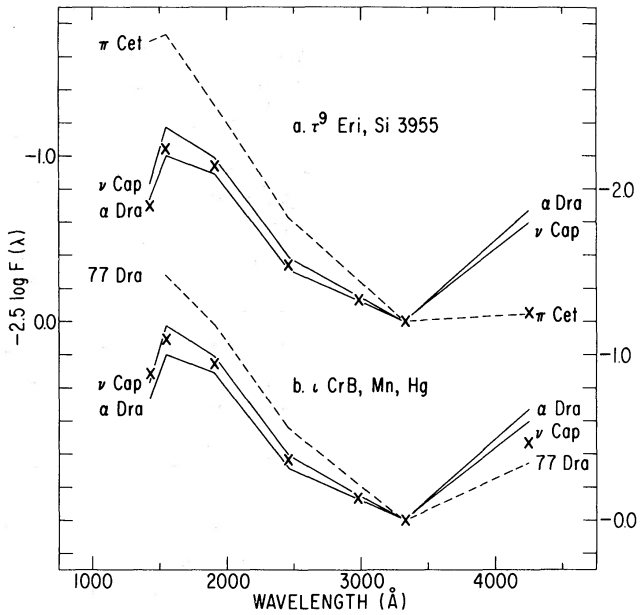

FIG. 5.—Format and symbols same as in fig. 3. (*a*) τ^9 Eri, ordinate axis labeled at left. τ^9 Eri (A0p) resembles π Cet (B7) in its *UBV* colors but possesses an ultraviolet flux distribution resembling those of ν Cap (B9.5) and α Dra (A0). (*b*) ι CrB, ordinate axis labeled at right. The ultraviolet flux distribution of ι CrB (A0p) is similar to those of ν Cap (B9.5) and α Dra (A0), although ι CrB has *UBV* colors like those of 77 Dra (B8).

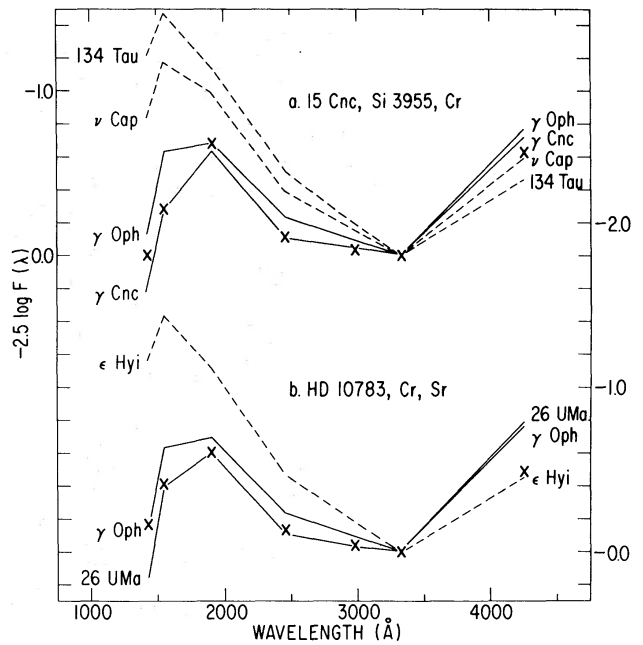

FIG. 6.—Format and symbols same as in fig. 3. (*a*) 15 Cnc, ordinate axis labeled at left. 15 Cnc (B9p) has *UBV* colors similar to those of 134 Tau (B9) and ν Cap (B9.5), but its ultraviolet flux distribution resembles those of early A stars like γ Cnc (A1). The MK class of 15 Cnc listed in table 5 would imply a nonexistent discrepancy between *UBV* color and spectral class for this Si star (see discussion in § IV). (*b*) HD 10783, ordinate axis labeled at right. The ultraviolet flux distribution of HD 10783 (A2p) resembles those of early A stars like γ Gem (A1) or 26 UMa (A2), although it possesses *UBV* colors like those of ϵ Hyi (B9).

TABLE 5

CLASSIFICATION OF Ap STARS ON THE BASIS OF THEIR ULTRAVIOLET FLUX DISTRIBUTIONS

Name or HD	*UBV* Comparison Stars*	*UBV* Class†	Ultraviolet Comparison Stars‡	Ultraviolet Class	MK Class	MK Class Source§
α And.....	α Col	B6–B7	134 Tau	B9	B9p	*a*
10783.....	ϵ Hyi	B9	γ Gem, 26 UMa	A1	A2p	*b*
τ^9 Eri.....	π Cet	B6–B7	ν Cap, α Dra	B9.5	A0p	*b*
32650.....	α Col, κ Lep	B7–B8	ϵ Hyi, ν Cap	B9–B9.5	B9p	*a*
μ Lep.....	α Col, κ Lep	B7	134 Tau	B9	B9p	*a*
34452.....	ι Her, δ For	B3–B5	134 Tau, ν Cap	B9.5	A0p	*a*
137 Tau.....	δ Cyg, α Dra	B9–B9.5	γ Oph	A0	B9p	*a*
θ Aur.....	134 Tau	B8–B9	γ UMa, γ Gem	A0–A1	A0p	*a*
15 Cnc.....	ϵ Hyi	B8–B9.5	γ Oph, γ Cnc	A1	B9p	*a*
49 Cnc.....	β CMi	B8	γ Cnc, 26 UMa	A1–A2	A1p	*a*
κ Cnc.....	α Col	B7	ϵ Hyi	B9	B8p	*b*
89822.....	134 Tau	B9	α Dra	B9.5–A0	A0p	*a*
α^2 CVn.....	κ Lep	B7–B8	α Dra, γ UMa	A0	A0p	*a*
84 UMa.....	ϵ Hyi	B9	γ Gem, 26 UMa	A1–A2	B9p	*a*
133029.....	β CMi	B8	γ Oph, γ Cnc	A1	B9p	*a*
ι CrB.....	77 Dra, 134 Tau	B9	ν Cap, α Dra	B9.5	A0p	*a*
υ Her.....	κ Lep	B7–B8	134 Tau, λ Cnc	B9–B9.5	B9p	*a*
149822.....	77 Dra, 134 Tau	B8–B9	δ Hyi	later than A2	B9p	*a*
46 Dra.....	κ Lep	B7–B8	134 Tau, λ Cnc	B9–B9.5	B9.5p	*a*
4 Cyg.....	α Col	B7	ϵ Hyi	B9	B9p	*a*
184905.....	β CMi	B8	δ Cyg	B9.5–A0	A0p	*b*
196178.....	τ Her	B5	77 Dra, ϵ Hyi	B8–B9	B9p	*a*
20 Cap.....	ι Lep, π Cet	B7	ν Cap, δ Cyg	B9.5	B9p	*a*
108 Aqr.....	δ For, π Cet	B5–B7	λ Cnc	B9.5	B9p	*a*

* Normal stars listed in tables 2 and 4 with *UBV* colors similar to those of the Ap star in question.

† Based on colors given in table 1 and Johnson's 1963 standard sequence.

‡ Normal stars listed in tables 2 and 4 with ultraviolet flux distributions closely resembling that of the Ap star in question.

§ *a*, Cowley *et al.* 1969; *b*, Jaschek *et al.* 1964.

All of the Ap stars considered here, except HD 149822, possess ultraviolet classes falling within the range B8–A2, the same range covered by their published MK types. Nineteen of these 23 stars have ultraviolet classes which agree with the MK classes listed for them in table 5 to within plus or minus one subclass—that is, to within the classification uncertainty. If one considers only those 19 Ap stars in table 5 for which the highly self-consistent study of Cowley *et al.* (1969) provides MK types, then agreement between ultraviolet and MK classes is obtained in 15 cases. The four exceptions —137 Tau, 15 Cnc (fig. 6*a*), 84 UMa, and HD 133029—are classified B9 by Cowley *et al.* but possess ultraviolet classes ranging from A0 to A2. All four of these stars occupy positions in the color-color diagrams of figures 1 and 2 consistent with other Ap stars of similar *UBV* colors and peculiarity classes. Thus, the discordance between their MK and ultraviolet classes probably reflects ambiguities in their MK types rather than anomalously cool ultraviolet color temperatures. Had the inhomogeneous compilations of Bertaud (1959) or Jaschek *et al.* (1964) been used as the primary source of MK types, agreement between ultraviolet and MK classes would have been obtained for virtually all of the Ap stars. The Ap stars considered possess HD classes B9 or A0. A consistent transfer of the present ultraviolet classes to the HD system results in B9–A0 ultraviolet classes for all of them.

The tightness of the agreement between MK and ultraviolet classes for the blue Ap

stars is somewhat surprising in light of the difficulties of classifying Ap star spectra. Osawa (1965) and others have shown that different classification criteria can yield different results for a given star. Classes derived from the Ca II K-line or from the He I lines do not necessarily describe the metallic line spectra or the strengths of the Balmer lines, for example. The problems are compounded by the ambiguities encountered in the use of certain criteria, e.g., in distinguishing between weak He I lines and blends of metallic lines on low-dispersion spectra. In the present context it must be emphasized that the MK classes listed in table 5 principally reflect the observed K-line strengths of the blue Ap stars. They also reflect, at least implicitly, weak or absent He I lines. These are among the standard criteria for late B and early A stars on the MK and HD systems, and they are the criteria in terms of which the classical discrepancies between *UBV* color and spectral type for blue Ap stars have been defined.

Most of the Ap stars listed in table 5 are too blue in $B - V$ for their published MK types. Color-spectral type discrepancies as large as 0.6 spectral classes are represented. A noteworthy result of the present study is that no such discrepancies between color and spectral type are evident at wavelengths shortward of 3320 Å. The Ap stars with large discrepancies between *UBV* color and MK class invariably resemble normal stars of similar MK class in the ultraviolet. One should not conclude from this empirical result that the blue Ap stars are simply like normal late B or early A stars, consistent with their MK types, either in terms of their effective temperatures or in terms of their atmospheric structure. A large body of evidence to the contrary exists. However, the present results do indicate that the blue Ap stars are not normal for their *UBV* colors either. Moreover, the agreement between their ultraviolet and MK classes is sufficiently tight as to suggest that their MK classes are not entirely the accidental result of atmospheric abundance anomalies in He and Ca, for example, but may result at least in part from other physical mechanisms, related to the temperature-pressure-radiation structure of their atmospheres.

V. ULTRAVIOLET SPECTROPHOTOMETRY OF θ AURIGAE

The observational results discussed in § IV are based entirely upon broad-band filter photometry. Such photometry, though useful in delineating general trends, is not an adequate substitute for higher-resolution ultraviolet spectrophotometry of the stars in question. There is cause for concern, for example, that the apparent ultraviolet flux deficiencies of the blue Ap stars in the broad-band data may merely reflect the presence of a few very strong absorption lines, lying near the center of each bandpass, and may not accurately characterize the overall ultraviolet flux envelopes of these stars.

Fortunately, a few of the Ap stars listed in table 1 are sufficiently bright to have been observable with the WEP spectrometers (Code *et al.* 1970). The silicon star θ Aur was reasonably well observed both with Spectrometer 1 (Sp 1) at about 20 Å resolution and with Spectrometer 2 (Sp 2) at about 10 Å resolution. Data for θ Aur and for some normal comparison stars are illustrated in figures 7 and 8. Also shown are the nominal half-power bandwidths of several WEP broad-band filters. The spectrometer data have been reduced only to the degree necessary for simple relative photometry. Apparent count rates were corrected for dark background, placed in magnitude units, and normalized to zero magnitudes at 3320 Å in the case of Sp 1, or to $U = 0.00$ in the case of Sp 2.

Spectrometer data of this sort are not available for all of the normal comparison stars observed with the broad-band filters. Among the normal stars represented in the Sp 1 data collection, ι And is the closest to θ Aur in its *UBV* colors. From the broad-band data of figure 1, one would expect ι And to be relatively brighter than a normal star with $U - V$ *identical* to that of θ Aur by less than 0.1 mag at 1910 and 2460 Å.

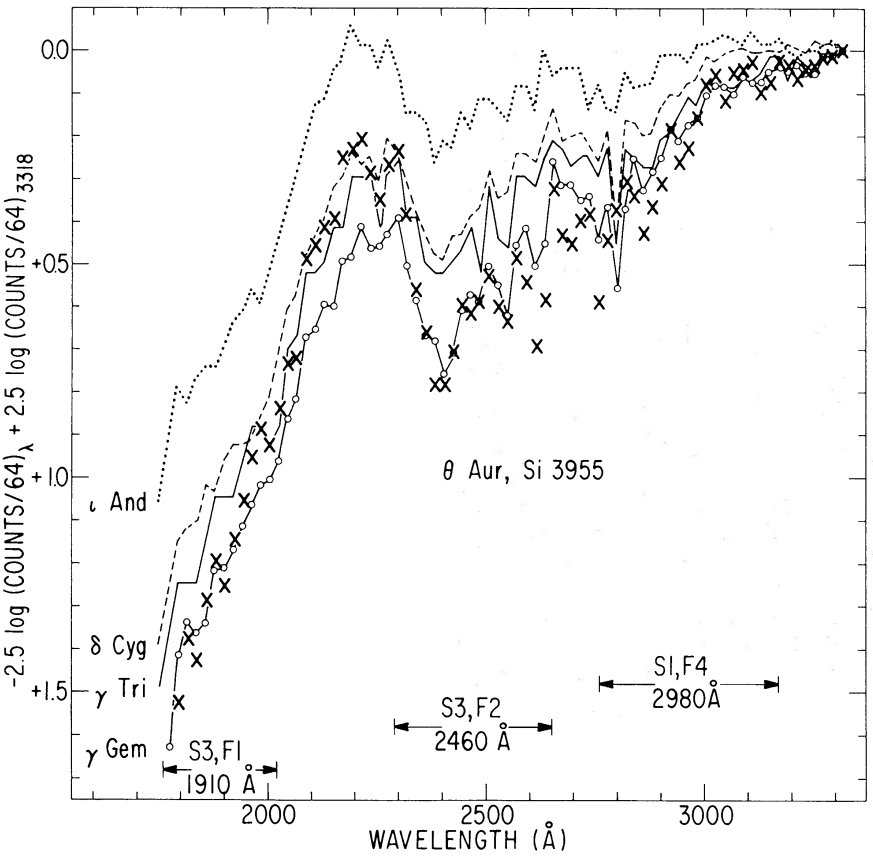

FIG. 7.—WEP Spectrometer 1 scans of θ Aur, denoted by crosses, and four normal comparison stars. Dotted lines connect data points for ι And (B8), a star with *UBV* colors approximating those of θ Aur (see discussion in § V). Data points for δ Cyg (B9.5), γ Tri (A1), and γ Gem (A1) are respectively connected by dashed lines, solid lines, and solid lines with open circles. The 20 Å bandpass data are normalized to zero magnitudes at 3318 Å. Half-power bandpasses of three WEP filters are shown. At no point does θ Aur approach in relative brightness a normal star of similar *UBV* colors, but it differs in detail from all normal stars shown.

Similarly, in the broad-band data β CMi is only 0.02 mag brighter at 1550 Å, relative to 3320 Å, than 134 Tau, the *UBV* comparison standard used for θ Aur in figure 3*b*. On this basis, ι And and β CMi adequately approximate normal stars with *UBV* colors like those of θ Aur over the wavelength ranges relevant to figures 7 and 8, respectively.

The Sp 1 and Sp 2 data generally confirm at higher resolution the trends noted in the broad-band data plotted in figure 3*b*. Note, for example, that data for θ Aur in the vicinity of 1500–1600 Å are bracketed by comparable data for the early A stars γ UMa and γ Gem in both figure 3*b* and figure 8. At no point over the wavelength range 1500–3000 Å does θ Aur approach in relative brightness normal stars of similar *UBV* colors.

Interesting differences in the point-by-point structure of the spectrometer scans between θ Aur and the normal stars are evident in figures 7 and 8. Some absorption features appear to be enhanced in θ Aur between 2300 and 3000 Å and also at 1720 Å. Enhanced line opacity from the third and fourth spectra of the rare earths may be responsible for some of the strong absorption features seen in the 2300–3000 Å interval (Dieke, Crosswhite, and Dunn 1961; Wolff and Wolff 1971), although θ Aur is not reported in the literature to be a strong rare earth star in the sense of α^2 CVn, for

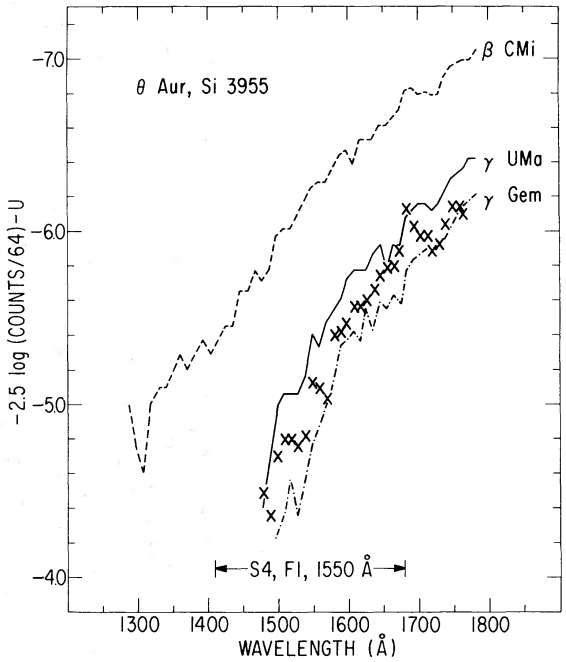

FIG. 8.—WEP Spectrometer 2 scans of θ Aur, denoted by crosses, and three normal comparison stars. Dashed lines connect data points for β CMi, a star which differs insignificantly from θ Aur in its UBV colors. Solid lines and dash-dot lines connect data points for γ UMa (A0) and γ Gem (A1), respectively. The 10 Å bandpass data are normalized to $U = 0.00$ mag. The half-power bandpass of the 1550 Å WEP filter is shown. θ Aur data are bracketed by data for γ UMa and γ Gem both here and in comparable broad-band data in fig. 3*b*. At no point does θ Aur approach in relative brightness a normal star of similar *UBV* colors.

example. Underhill, Leckrone, and West (1972) have shown that the as yet unidentified feature at 1720 Å is a good indicator of stars with extended atmospheres. It is present in great strength in spectra of early-type supergiants and shell stars but is weak or absent in the spectra of dwarfs and giants. It is noteworthy that the 1720 Å feature is as strong in the spectrum of θ Aur as it is in supergiant or shell-star spectra. The feature which is commonly *assumed* to be the Mg II 2800 Å resonance doublet in Sp 1 scans of normal stars does not appear in the scan of θ Aur shown in figure 7, or at least it is too weak to be resolved here, although it is evident in the comparison star scans illustrated.

There is no compelling evidence in the scan of θ Aur shown in figure 8 for the presence of the Si I ionization edges at 1520 and 1680 Å with strengths greater than their strengths in normal stars. The weak (about 0.1 mag) 1680 Å edge identified by Molnar (1973) in α^2 CVn may be present also in θ Aur *and* in the normal stars illustrated here, but this is difficult to determine with certainty. The wavelength region near 1680 Å is complicated by the apparent presence of absorption lines both in θ Aur and in normal stars. Also, low weight must be given to the θ Aur data point at 1683 Å, there being substantial scatter at this single point between the two Sp 2 scans averaged for illustration in figure 8.

VI. THE EFFECTIVE TEMPERATURE OF HR 1732

The derivation of accurate effective temperatures and bolometric corrections for both the blue Ap stars and the normal comparison stars included in this study is hampered by uncertainties in the calibration of the ultraviolet data, the lack of observations or suitable theoretical flux distributions covering wavelengths shortward of

1430 Å, and the lack of spectral energy distribution data longward of 3300 Å for many of the stars of interest. However, a crude estimate of the *difference* in effective temperature between one of the blue Ap stars and a normal B star of similar $B - V$ color may prove instructive.

One of the bluest known Si stars, HR 1732, resembles the normal B3 V star ι Her in its *UBV* colors. Effective-temperature estimates from ground-based model atmospheres analyses (Peters and Aller 1970; Tomley, Wallerstein, and Wolff 1970), when consistently placed on a scale defined by line-blanketed models, are closely similar for the two stars. However, the ultraviolet flux deficiency of HR 1732 relative to ι Her (fig. 4*a*) implies that the former is in reality cooler than the latter. If one assumes that ι Her and HR 1732 emit identical fluxes at wavelengths greater than or equal to 3320 Å, as discussed in § IV, and that fluxes emitted in the Lyman continua of both stars are negligible, then their effective temperatures T_e are related by

$$(T_e^4)_{\iota\ \mathrm{Her}} - (T_e^4)_{1732} \simeq \frac{\pi}{\sigma} \int_{912\ \text{Å}}^{3320\ \text{Å}} [f_\lambda(\iota\ \mathrm{Her}) - f_\lambda(1732)]d\lambda\,, \tag{4}$$

where σ is the Stefan-Boltzmann constant and f_λ is emergent flux as defined in § IV. Let it further be assumed, following Peters and Aller (1970), that ι Her is reasonably well represented by the $T_e = 16{,}800°$ K model of Adams and Morton (1968), which may be used to establish the flux-scale zero point at 3320 Å for both stars (Van Citters and Morton 1970). Flux distributions over 1430–3320 Å are then obtained from table 4. The unobserved 912–1430 Å region for ι Her may be represented by the Adams-Morton model fluxes, while the HR 1732 flux distribution may be crudely extrapolated in shape to the Lyman limit by use of the predicted ultraviolet flux distribution of a Klinglesmith (1971*b*) model atmosphere ($T_e = 11{,}000°$ K, $\log g = 4.0$). Implicit in the latter procedure is the assumption that HR 1732 continues to resemble a normal late B-type star like ν Cap from 1430 Å to the Lyman limit, analogous to the close resemblance found from 3320 to 1430 Å. Application of these assumptions in equation (4) yields $T_e \simeq 14{,}500°$ K for HR 1732, or an effective-temperature difference $\Delta T_e \approx 2300°$ K between ι Her and HR 1732. Reasonable alternative choices of assumed T_e for ι Her or of extrapolation procedures shortward of 1430 Å result in values of ΔT_e differing from the one quoted above by about $\pm 300°$ K. In summary, although HR 1732 closely resembles a B3 or B4 star in terms of its *UBV* colors and other ground-based observables, its effective temperature could in fact be as cool as that of a normal B6 star.

It was shown in § IV that the Hg-Mn stars are less flux-deficient in the ultraviolet for their *UBV* colors than are the Si stars. Calculations for Hg-Mn stars of the sort outlined above would therefore yield much smaller effective-temperature defects, ΔT_e, relative to normal stars of like *UBV* colors. Consequently, the Si and the Hg-Mn stars must overlap more strongly in the (T_e, $\log g$)-plane than has previously been supposed (see, e.g., Jugaku and Sargent 1968, fig. 3).

VII. DISCUSSION

The ultraviolet data for the blue Ap stars suggest the presence of enhanced ultraviolet line and continuum opacity sources, distributed continuously and more or less uniformly from about 3000 Å to the shortest wavelength observed, 1430 Å. It is to be expected that elements with enhanced line strengths at visible wavelengths in Ap stars will also exhibit abnormally strong lines and continua in the ultraviolet, and these include metallic species with very rich ultraviolet spectra. The Hg-Mn stars, which exhibit fewer line-strength anomalies in the visible, are also less flux-deficient in the ultraviolet than are Si or Sr-Cr-Eu stars. The ultraviolet flux emerging from an Ap

star's atmosphere must originate closer to the boundary of that atmosphere than is the case in normal stars of the same effective temperature. Thus, the observed ultraviolet flux distribution of an Ap star could mimic that of a normal star of cooler effective temperature. It is not clear, however, why the cooler normal star and the blue Ap star in question should possess essentially identical MK spectral types, as is observed in most cases.

The full impact of greatly enhanced ultraviolet opacities and strong magnetic fields on the atmospheric structure of an Ap star must be established. An obvious, but by no means simple, first step is the calculation of fully blanketed model atmospheres with assumed elemental abundances of the sort deduced for Ap stars from ground-based spectra. The problem is iterative in that the heavily blanketed models so derived should be used to reevaluate the elemental abundances.

At depth an atmosphere with enhanced ultraviolet opacities should resemble in its temperature-pressure structure a less heavily blanketed atmosphere of hotter effective temperature. The situation in shallower layers is complicated by the details of the assumed line formation mechanism (Mihalas 1970, chapter 14). However, for heuristic argument let it be assumed that (1) a heavily blanketed atmosphere and the hotter normal atmosphere it resembles at depth diverge in their T-P structure at small standard optical depths, the divergence possibly being accentuated by the presence of strong magnetic fields in the heavily blanketed atmosphere, and (2) the stronger the enhancement of ultraviolet opacities (and possibly the stronger the magnetic field), the greater will be this divergence. Under these circumstances observables originating at depth—e.g., the Paschen continuum and the Balmer line wings—will be closely similar for the two atmospheres, but spectral features formed in shallower layers may be dissimilar in the two cases. In particular if the indicators of spectral type, such as the strong He I lines or the Ca II K-line, are formed in regions where the heavily blanketed and the corresponding normal atmospheres differ, the result would be apparent discrepancies between UBV color and spectral type. The Hg-Mn stars, being less heavily blanketed and possessing weak or nonexistent magnetic fields, would typically possess smaller discrepancies between color and spectral type than Si stars, as is observed to be the case.

Two examples of the mechanism outlined above will suffice to illustrate its possible importance in the interpretation of Ap star spectra. In analyses of three Mn stars, K. M. Strom (1969) found that a $T_e = 11{,}000°$ K LTE model atmosphere with enhanced Si I ultraviolet opacity and a 12,000° K normal model both matched the stars in question in terms of the Balmer discontinuity, the Paschen slope, and the Balmer line wings. However, the silicon-rich model predicted weaker He I λ4471 equivalent widths for a given assumed He/H ratio than did the normal model. Helium abundances derived with the enhanced opacity model were larger than those given by the normal model by factors of 2 or 3. Second, two LTE model atmospheres calculated by Fowler (1972, 1973)—a fully line-blanketed model with $T_e = 9700°$ and a $T_e = 10{,}300°$ K model with hydrogen line blanketing only—each matched the observed Balmer discontinuity, Paschen slope, and Balmer line wings of Sirius. Each model predicted the same equivalent width of Fe II λ4631.9 for a given Fe/H ratio, but the fully blanketed model yielded an equivalent width for Fe I λ3581.2 significantly larger than that given by the partially-blanketed model. Apparently the Fe I line is formed high in the atmosphere where the two models differ in predicted degree of Fe I ionization. Fowler obtained Fe II/Fe I ionization balance for a unique assumed Fe/H ratio for Sirius with the fully blanketed model but found a wide disparity between Fe/H ratios derived with these two Fe I and Fe II lines predicted by the partially blanketed model. It thus appears possible that some anomalies in the spectra of Ap stars previously attributed to abundance effects may arise at least in part as a consequence of dissimilarities in overall atmospheric structure between Ap and normal stars, produced

by enhanced ultraviolet opacities in the former. Meaningful discussions of the origin of abundance anomalies in Ap stars will depend upon the disentanglement of real abundance peculiarities from such atmospheric structure effects.

The author is indebted to A. D. Code of the University of Wisconsin for the opportunity to use the Wisconsin Experiment Package on OAO-2 and data obtained therefrom. The assistance of A. V. Holm of the University of Wisconsin, J. J. Caldwell of Princeton University, and S. R. Heap, W. M. Sparks, and D. K. West of the Goddard Space Flight Center is gratefully acknowledged. Thanks must also be extended to J. F. McNall of the University of Wisconsin and to M. R. Molnar of LASP for valuable comments and discussion.

REFERENCES

Abt, H. A., and Snowden, M. S. 1973, *Ap. J. Suppl.*, **25**, 137.
Adams, T. F., and Morton, D. C. 1968, *Ap. J.*, **152**, 195.
Batten, A. H. 1967, *Pub. Dom. Ap. Obs.*, **13**, 119.
Bernacca, P. L., and Molnar, M. R. 1972, *Ap. J.*, **178**, 189.
Bertaud, C. 1959, *J. d. Obs.*, **42**, 45.
Blanco, V. M., Demers, S., Douglass, G. G., and Fitzgerald, M. P. 1968, *Pub. Naval Obs.*, **21**, 1.
Bless, R. C., and Savage, B. D. 1972, *Ap. J.*, **171**, 293.
Code, A. D. 1969, *Pub. A.S.P.*, **81**, 475.
———. 1971, private communication.
Code, A. D., Houck, T. E., McNall, J. F., Bless, R. C., and Lillie, C. F. 1970, *Ap. J.*, **161**, 377.
Conti, P. S. 1970, *Ap. J.*, **160**, 1077.
Cowley, A., Cowley, C., Jaschek, M., and Jaschek, C. 1969, *A.J.*, **74**, 375.
Deutsch, A. J. 1947, *Ap. J.*, **105**, 283.
Dieke, G. H., Crosswhite, H. M., and Dunn, B. 1961, *J. Opt. Soc. Am.*, **51**, 820.
Dworetsky, M. M. 1972, private communication.
Eggen, O. J. 1967, in *The Magnetic and Related Stars*, ed. R. C. Cameron (Baltimore: Mono Book Corp.), p. 141.
Fowler, J. W. 1972, *Line Blanketed Model Stellar Atmospheres Applied to Sirius*, NASA Publication X-670-72-303.
———. 1973, private communication.
Hiltner, W. A., Garrison, R. F., and Schild, R. E. 1969, *Ap. J.*, **157**, 313.
Hoffleit, D. 1964, *Catalogue of Bright Stars* (New Haven: Yale University Observatory).
Hyland, A. R. 1967, in *The Magnetic and Related Stars*, ed. R. C. Cameron (Baltimore: Mono Book Corp.), p. 311.
Jaschek, C., Conde, H., and de Sierra, A. C. 1964, *Catalogue of Stellar Spectra Classified in the Morgan-Keenan System* (LaPlata Observatory).
Johnson, H. L. 1963, in *Basic Astronomical Data*, ed. K. Aa. Strand (Chicago: University of Chicago Press), p. 204.
Johnson, H. L., Mitchell, R. I., Iriarte, B., and Wisniewski, W. Z. 1966, *Comm. Lunar and Planet. Lab.*, **4**, 99.
Jugaku, J., and Sargent, W. L. W. 1968, *Ap. J.*, **151**, 259.
Klinglesmith, D. A. 1971*a*, private communication.
———. 1971*b*, *Hydrogen Line Blanketed Model Stellar Atmospheres*, NASA SP-3065.
———. 1972, private communication.
Mihalas, D. 1970, *Stellar Atmospheres* (San Francisco: W. H. Freeman & Co.).
Mihalas, D., and Henshaw, J. L. 1966, *Ap. J.*, **144**, 25.
Molnar, M. R. 1973, *Ap. J.*, **179**, 527.
Osawa, K. 1965, *Ann. Tokyo Astr. Obs.*, 2d Ser., **9**, 123.
Peters, G. J., and Aller, L. H. 1970, *Ap. J.*, **159**, 525.
Peterson, D. M. 1970, *Ap. J.*, **161**, 685.
Preston, G. W. 1970, in *Stellar Rotation*, ed. A. Slettebak (Dordrecht: Reidel), p. 254.
———. 1971, *Pub. A.S.P.*, **83**, 571.
Sargent, W. L. W., and Searle, L. 1967, in *The Magnetic and Related Stars*, ed. R. C. Cameron (Baltimore: Mono Book Corp.), p. 209.
Searle, L., and Sargent, W. L. W. 1964, *Ap. J.*, **139**, 793.
Stępień, K. 1968*a*, *Ap. J.*, **153**, 165.
———. 1968*b*, *ibid.*, **154**, 945.
Strom, K. M. 1969, *Astr. and Ap.*, **2**, 182.
Strom, S. E., and Strom, K. M. 1969, *Ap. J.*, **155**, 17.

Tomley, L. J., Wallerstein, G., and Wolff, S. C. 1970, *Astr. and Ap.*, **9**, 380.
Underhill, A. B., Leckrone, D. S., and West, D. K. 1972, *Ap. J.*, **171**, 63.
Van Citters, G. W., and Morton, D. C. 1970, *Ap. J.*, **161**, 695.
Wolff, S. C., and Wolff, R. J. 1971, *A.J.*, **76**, 422.

Note added in proof.—The relative absolute fluxes defined by equation (3) and tabulated in table 4 refer to fluxes per unit wavelength interval. Although a preliminary flux calibration has been applied to these data, the results of the program of *relative* photometry outlined in § IV are independent of the calibration.